

Transition-metal dioxides with a bulk modulus comparable to diamond

Urban Lundin, Lars Fast, Lars Nordström, and Börje Johansson

Condensed Matter Theory Group, Department of Physics, University of Uppsala, Box 530, S-751 21 Uppsala, Sweden

J. M. Wills

Theoretical Division, Los Alamos National Laboratory, Los Alamos, New Mexico 87545

Olle Eriksson

Condensed Matter Theory Group, Department of Physics, University of Uppsala, Box 530, S-751 21 Uppsala, Sweden

and Theoretical Division, Los Alamos National Laboratory, Los Alamos, New Mexico 87545

(Received 22 October 1997)

Recently it has been reported that a high-pressure cubic phase of ruthenium dioxide has an unusually large bulk modulus, and consequently is a most interesting candidate as a very hard material. Based on *ab initio* calculations it is shown that the high bulk modulus is a result of a strong covalent bonding between ruthenium *d* states and oxygen *p* states in combination with the favorable geometry of the orbitals in the fluorite structure. In addition an even higher bulk modulus is predicted for the isoelectronic and isostructural compound OsO₂. [S0163-1829(98)07209-9]

Hard materials have been studied for a long time both experimentally and theoretically due to their wide range of important technological applications.¹ Although hardness is a macroscopic phenomena, the microstructure, such as bonds and atomic size, is very important for the measured strength of a material. As an example, the general explanation for why diamond is the hardest material observed today is that directed covalent *sp*³ bonds between the carbon atoms give rise to a very rigid and hard structure.² Even a small deformation requires a lot of energy due to the strength of the carbon-carbon bond. Although diamond is not especially close packed it is, due to the rigidity of its covalent bonds, harder than all other presently known materials. Other examples of hard materials are the cubic BN and the hexagonal WC compounds.¹

The hardness is measured by making an indent in the material and measure its size. The difficulty in calculating hardness directly has led scientists to look for an additional measure of hardness. A good and frequently used candidate for this is the bulk modulus, which reflects the volume stiffness of the lattice.¹⁻³ In a plot of hardness versus bulk modulus one sees a strong correlation between the two.⁴ For non-cubic systems the shear modulus may be a more precise measure of the hardness. However, for cubic systems the bulk modulus should be a quite good indicator of hardness.

In this paper we investigate a class of candidate hard materials; transition-metal dioxides in the cubic-CaF₂ structure. According to experiments⁵ there is a structural transition in RuO₂ from the ground state rutile phase to an orthorhombic distortion of the rutile phase at a pressure of 8 GPa and a second transition to the cubic fluorite phase at 12 GPa. In a later paper⁶ this structure was reported as a distorted fluorite phase, where the Ru-O distance ($=u$), is different from the ideal value 1/4. We have investigated also this phase, and it will be discussed below. This high-pressure phase is metastable at ambient conditions, with a very high bulk modulus 399 GPa (Refs. 4 and 5) at zero pressure. The possibility to

stabilize cubic RuO₂ at ambient conditions, for instance by epitaxial growth on a cubic substrate, could open avenues for ultrahard materials to be used in applications. We have investigated this experimental finding on RuO₂ by means of first-principles calculations, which confirm the experimentally found extreme behavior of RuO₂. Further, we analyze the origin of the hard chemical bonds of this material, and study other related compounds within the same crystal structure. Most notably we predict OsO₂ to be very stiff, with a bulk modulus of 411 GPa, which is actually higher than for cubic BN.

Using a full-potential linear muffin-tin orbital method⁷ (FP-LMTO) we have calculated the total energy as a function of volume for a number of selected transition-metal dioxides, which are likely to show a high bulk modulus, in the CaF₂ structure. The calculations were based on the local-density approximation (LDA) of the density functional theory. The unit cell was divided around the atoms into non-overlapping muffin-tin spheres, in which the basis functions were expanded in spherical harmonics up to a cutoff in angular momentum, $l_{\max}=6$. The basis functions in the interstitial region were Neuman or Hankel functions. In the calculations for RuO₂ we included the Ru *4p*, *5s*, *5p*, and *4d* orbitals and the O *2s*, *2p*, and *3d* orbitals in the basis. Similar basis sets were used for the other studied systems.

As a precursor to the main investigation we studied the phase stability between the ideal and distorted fluorite phases. Calculations where the Ru-O distance was optimized showed an energy barrier between the fluorite structure ($u=0.25$) and the experimentally obtained distorted fluorite phase ($u=0.347$).⁶ This energy barrier could explain the fact that the distorted phase is found in some experiments, and the ideal fluorite in others. Since we have applications in mind in our study, where hopefully RuO₂ could be deposited on a cubic compound, thus making the ideal fluorite possible, we will for the rest of the paper ignore the distorted phase.

The fluorite structure has an fcc Bravais lattice with a

TABLE I. Bulk moduli B_{theory} and B_{exp} for the selected compounds. Lattice parameter a_{theory} .

Material	a_{theory} (a.u.)	B_{theory} (GPa)	B_{exp} (GPa)
Diamond	6.70	452	443 ^a
RuO ₂	8.99 ^c	343	399 ^b
RuNF	9.08	396	
OsO ₂	9.00	411	
OsNF	9.21	315	

^aFrom Ref. 9.

^bFrom Ref. 4.

^cThe experimental lattice parameter was 8.933 a.u. at 40 GPa and 9.139 a.u. at ambient conditions.

basis of metal atoms positioned at (0,0,0) and ligand atoms positioned at $\pm(1/4,1/4,1/4)$ in units of the lattice constant. The transition-metal atom has an octahedral environment with eight ligand atoms as nearest neighbors, while the ligand atoms are positioned at tetrahedral sites with four metal atoms as nearest neighbors. This structure can in fact be related to the diamond structure. If the atoms would be of the same type, the fluorite structure is constructed from the diamond structure by filling its open void at $(-1/4,-1/4,-1/4)$ with an extra atom. This leaves the ligand atoms of the CaF₂ structure with a diamondlike set of nearest neighbors whereas the metal atoms have a more close packed octahedral surrounding.

The calculated total energy E as a function of volume V was fitted to an integrated form of the Birch⁸ equation of state, from which the bulk modulus was extracted as $B = V_0(d^2E/dV^2)_{V_0}$, where V_0 is the equilibrium volume.

The calculated bulk modulus and lattice parameter for RuO₂ are in accordance with experiment, as can be seen in Table I. Deviations can be understood from the limitations of the LDA approximation.¹⁰ To explain the high values for the bulk modulus we investigate the bonding character of the material. The electronic structure of RuO₂ is governed by a strong hybridization between the Ru- d and O- p states as can be seen in the calculated density of states (DOS) shown in Fig. 1. The total DOS consists of energy bands separated into four groups. The two lowest $[(-0.7)-(-0.4)$ and $(-0.4)-(-0.1)$ Ry], containing 6+6 states, are dominated by O- p character but have a significant Ru- d contribution, while the two higher lying peaks are dominated by the Ru- d states with a rather small contribution from the O- p states, especially in the highest lying unoccupied bands. We have found that the two lowest features may be viewed as the bonding part of the hybridization complex formed by the nearest neighbor bonding O- p and Ru- $d_{t_{2g}}$ states, while the unoccupied highest lying feature is the corresponding antibonding part. The next highest lying narrow peak, which is the highest occupied region $[(-0.1)-(-0.0)$ Ry], is formed mainly by the, to first approximation, nonbonding Ru- d_{e_g} states, and contains four states.

This analysis is confirmed by the four orbital densities plotted in Fig. 2 for a (110) cut through both the Ru and O sites. The orbital densities were defined as

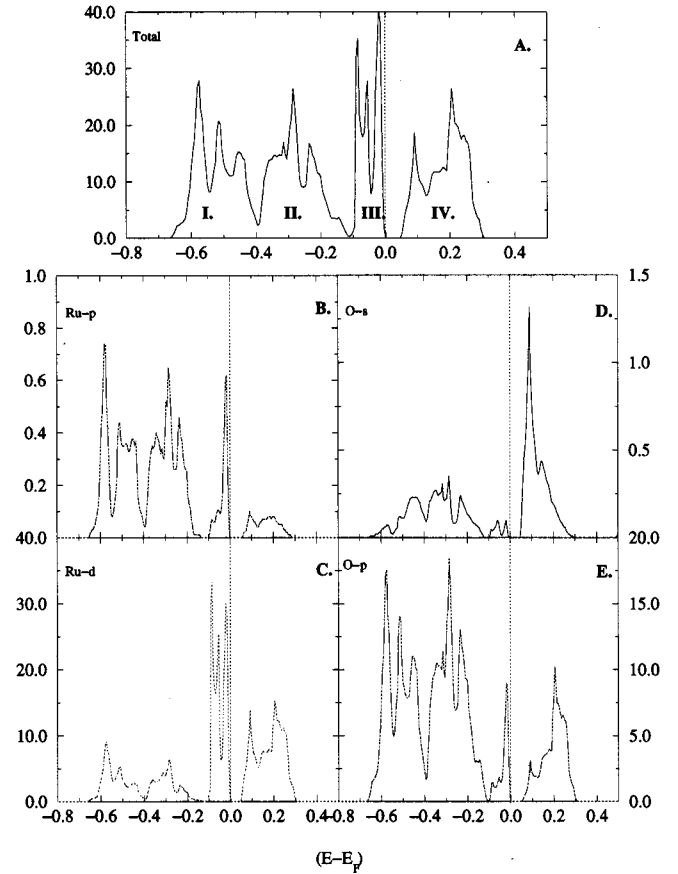


FIG. 1. The total and projected density of states for RuO₂. The Fermi level is indicated by a vertical dotted line. (A) shows the total DOS, (B) the p -projected Ru DOS, (C) shows the d -projected Ru DOS, (D) shows the s -projected O DOS, and (E) shows the p -projected O DOS.

$$\rho_j(\vec{r}) = \sum_{\epsilon_{A_j} \leq \epsilon_i \leq \epsilon_{B_j}} |\Psi_i(\vec{r})|^2, \quad (1)$$

where Ψ_i and ϵ_i are the eigenvector and eigenvalue of the state i , respectively, and ϵ_{A_j} and ϵ_{B_j} are the lower and upper energy limits defining the j th region in the DOS. The sum of the orbital densities from the three lowest regions is identical to the valence charge density. The orbital densities show the local space variation of the orbitals forming the electronic bands in the different parts of the energy spectrum. The two lowest lying regions have similar orbital densities, which both show the bonding between the O and Ru sites. The difference between these two can best be seen in the region between the two oxygen neighbors. Since the lowest region shows more O-O bonding orbital density and the second region shows a tendency towards a node between the O sites, the energy difference between these two regions might be viewed as an O-O bonding antibonding splitting. The third region shows a large density concentration around the Ru sites with orbitals pointing along the cubic crystal axes, not towards the O sites. This is in accordance with a density formed by local d_{e_g} orbitals. Finally, the fourth orbital density shows a clear node between the Ru and O sites typical for antibonding orbitals. In this orbital density we can also observe two additional features. The density between the

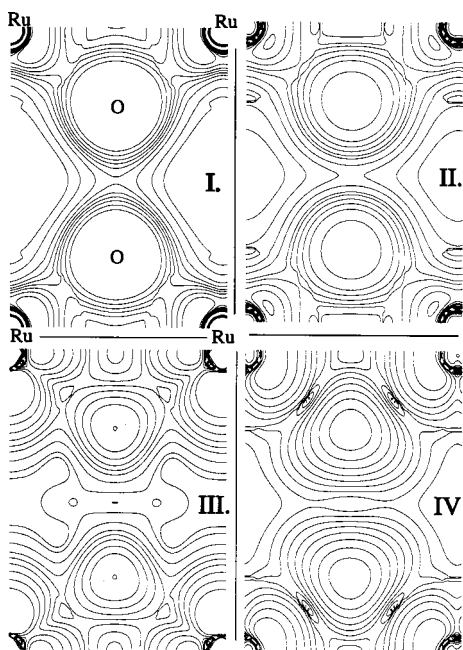


FIG. 2. The charge density for RuO_2 . (I) includes the valence charge derived from the energy region (0.7) to (0.4) Ry below the Fermi energy, i.e. region I in Fig. 1. In the same way (II) and (III) show the valence charge derived from regions II (-0.4) to (-0.1) Ry and III (-0.1) to (0.0) Ry, respectively. (IV) shows the orbital density for the energy region IV from (0.0) to (0.4) Ry. The plot is made in the (110) plane.

next nearest, i.e., oxygen, sites show an even more pronounced antibonding character than that of region II, and the orbital density around the O site has a clear tetrahedral form with lobes pointing in directions away from the Ru sites. One sees from symmetry that it is possible to form a density pointing towards the oxygen sites along the body diagonal from local linear combinations of $\text{Ru-}d_{t_{2g}}$ orbitals, which then can form directed bonds with the O states.

The obtained tetrahedrally formed orbital density cannot be obtained from p states alone, but it is well known that sp^3 hybrids form such densities. This fact leads directly to comparisons with diamond. However, they should not be carried too far, since, e.g., the bonding states which are responsible for the hard bonds have much weaker s character. One parallel is, however, that RuO_2 as well as diamond has an optimal number of valence electrons to occupy the bonding states, while leaving the antibonding states unoccupied. In the case of RuO_2 there is also an optimal energy separation between the O- p and Ru- d states to produce strong bonds without having to invoke a substantial charge transfer.

Besides studying RuO_2 we have performed similar calculations for the isostructural series MO_2 ($M = \text{all } 4d \text{ elements plus selected } 5d \text{ elements}$). The best covalent bonding properties are obtained for RuO_2 , because from this system all bonding states are filled. In the other $4d$ dioxides either antibonding states are filled (in the compounds to the right in the Periodic Table from Ru) or bonding or nonbonding states are drained (in the compounds to the left from Ru), which gives a parabolic trend in B for the $4d$ dioxides. This can be compared to the pure transition metals where the maximum bonding occurs in the middle of the series. In addition the

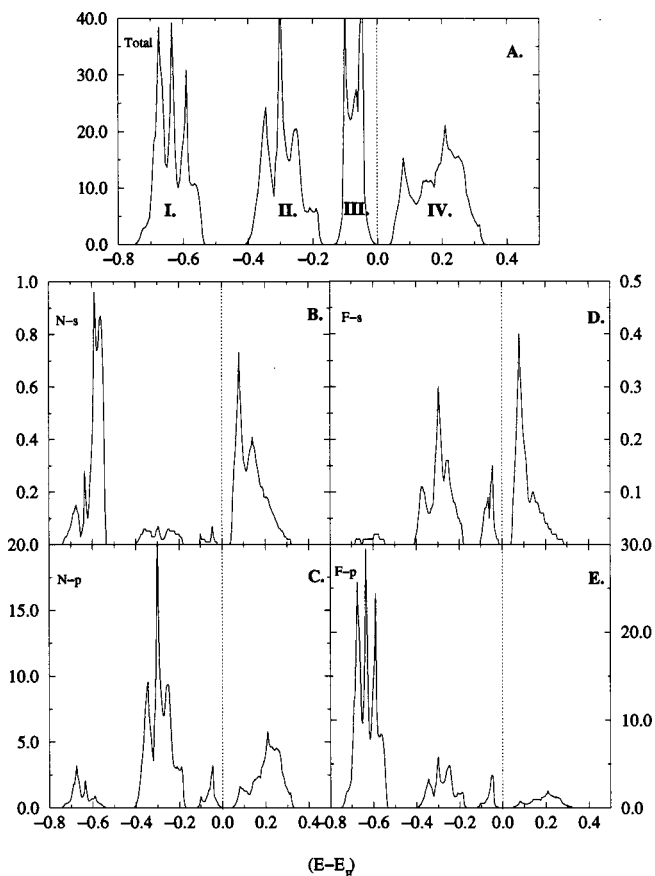


FIG. 3. The total and projected density of states for RuNF . The Fermi level is indicated by a vertical dotted line. (A) shows the total DOS, (B) the s -projected N DOS, (C) shows the p -projected N DOS, (D) shows the s -projected F DOS, and (E) shows the p -projected F DOS.

ionic contribution to the bonding in MO_2 is smallest for $M = \text{Ru}$, and increases when going either to the left or to the right in the $4d$ series. We have also calculated the compounds RuXY ($X, Y = \text{all pairs of } B \text{ to } F$). The result of these calculations is that the most favorable separation into bonding or antibonding is found for compounds isoelectronic to RuO_2 , this is discussed below.

Of special interest are the following two isovalent compounds: OsO_2 and RuNF . In the latter case the nitrogen and fluorine atoms occupy one each of the two originally identical ligand sites. Both these materials have a larger bulk modulus than RuO_2 . In the case of OsO_2 the physical picture is very much in parallel to the one above for RuO_2 . The calculated lattice constants and bulk moduli are given in Table I, and we note that OsO_2 is an even better candidate as a hard material. The electronic structure of RuNF is seen from the DOS in Fig. 3. The two lowest bonding peaks are now further split, compared to RuO_2 . The lower in energy (region I in Fig. 3) comes from Ru- d -F- p hybridization and the other (region II in Fig. 3) comes from the hybridization of Ru- d and N- p atomic orbitals. This picture is also verified from an orbital density plot, such as the one for RuO_2 , but since the plot is very similar to RuO_2 it is not shown here. Changing from Ru to Os increased the bulk modulus for the dioxide, and changing O_2 into NF also improved the bulk modulus. It would then be natural to assume that this last change would

improve also the Os compound. However, this was not the case, the bulk modulus decreased. This decrease can be traced back to the fact that the volume has been considerably increased.

Moreover, our theoretical analysis shows that the bonds are not ionic since, compared to the neutral atom, oxygen in the solid has *lost* some of its electrons to the bond between Ru and O. The occupation numbers in our first-principles theory should, however, not be taken too literally since they depend on how we define the base geometry (muffin-tin radii) of the system. However, for trends one can make use of these numbers. This, and the above discussion, demonstrate covalent nature of the bonds.

Our findings presented here are to be compared with the calculations made for hexagonal WC, where Liu *et al.*¹ analyzed the bonds as metallic between the metal atoms and partially ionic between the metal and the ligand. This conclusion was drawn when comparing the bcc W metal with the hexagonal WC crystal. In our present case, we find that for RuO₂ such a description does not lead to a proper picture. By analyzing our own calculations for WC, we find again that there is a considerable amount of covalent character in the bonding. This leads to a general consensus regarding how to achieve a large bulk modulus in transition-metal compounds.

(1) Optimal filling of the bonding orbitals formed by *d-p* hybridization in the metal-ligand system. Note that the relative positions of the *d* and *p* bands are important for an effective hybridization. Possible nonbonding states may be ignored.

(2) Little ionicity in the bonding. This could be understood from the fact that an ionic bond involves an extra degree of freedom, the charge transfer, which may change under pressure, relaxing the energy, and thereby soften the bond.

(3) The crystal structure should have as few internal parameters as possible. Since again, extra degrees of freedom,

which the system can use to relax and lower the total energy when subjected to compression, counteract high bulk modulus. Ideally good candidates should have, as the cubic systems studied here, an isotropic and symmetric (e.g., cubic) crystal structure.

As mentioned in the introduction, the ruthenium compound RuO₂ is metastable in the cubic fluorite structure at ambient pressure. Nevertheless it should not be too difficult to grow such a material. Due to the remarkable development in thin film fabrication and epitaxial growth, we speculate that it may be possible to stabilize films of these materials by means of growth on cubic substrates. If this could be achieved one would have a technologically very interesting system, a cubic substrate with a very hard coating on top. The fact that these materials are hard in a cubic phase is important also from the view point that this most often results in many different planes of deformation, ensuring good plastic behavior.

In summary we have calculated the electronic structure of a number of transition-metal dioxides in the fluorite structure and found that they have a very high bulk modulus. The optimal bulk modulus is found for the material OsO₂. This can be understood from the favorable conditions for strong covalent bonds for these materials. The calculated properties of RuO₂ are in good agreement with experiments. The highest bulk modulus found for materials in the CaF₂ structure is predicted to be 411 GPa for OsO₂. Since this material is closely related to RuO₂ it would be interesting to see if it transforms to the fluorite structure at high pressure. The high bulk modulus together with the fact that the fluorite structure is cubic, make this family of compounds particularly worthwhile for further studies, in the search for hard materials.

This project has been financed by the Swedish Natural Science Research Council (NFR), and Materials Consortium No. 9 (SFS).

¹A. Y. Liu, R. M. Wentzcovitch, and M. L. Cohen, *Phys. Rev. B* **38**, 9483 (1988).

²M. Ashizuka and M. Murkami, *J. Jpn. Inst. Metals* **53**, 88 (1989).

³H. Neumann, *Cryst. Res. Technol.* **23**, 97 (1988).

⁴J. M. Legér and B. Blanzat, *J. Mater. Sci. Lett.* **13**, 1688 (1994).

⁵J. Haines and J. M. Legér, *Phys. Rev. B* **48**, 13 344 (1993).

⁶J. Haines, J. M. Legér, and O. Shulte, *Science* **271**, 629 (1996).

⁷J. M. Wills (unpublished); J. M. Wills and B. R. Cooper, *Phys. Rev. B* **36**, 3809 (1987).

⁸F. Birch, *Phys. Rev.* **71**, 809 (1947).

⁹I. V. Aleksandrov, A. F. Goncharov, A. N. Zisman, and S. M. Stishov, *Sov. Phys. JETP* **66**, 384 (1987).

¹⁰Normally LDA underestimates the equilibrium volume, so that the bulk modulus is overestimated by about 6%. These shortcomings are usually cured by means of the so-called gradient corrected approximation. However, in the present work we are not interested in very accurate values of the bulk modulus but focus more on general trends, and therefore the LDA error is here only a minor inconvenience.